

# Electronic and Optical Properties of the TlInS<sub>2</sub> Crystal: Theoretical and Experimental Studies

T. BABUKA<sup>a,b,\*</sup>, O.O. GOMONNAI<sup>c,d</sup>, K.E. GLUKHOV<sup>a</sup>, L.YU. KHARKHALIS<sup>a</sup>,  
M. SZNAJDER<sup>e</sup> AND D.R.T. ZAHN<sup>f</sup>

<sup>a</sup>Institute for Physics and Chemistry of Solid State, Uzhhorod National University,  
54 Voloshin Str., 88000 Uzhhorod, Ukraine

<sup>b</sup>Institute of Physics, Faculty of Mathematics and Natural Science, Jan Długosz University in Częstochowa,  
Al. Armii Krajowej 13/15, PL-42200 Częstochowa, Poland

<sup>c</sup>Optics Department, Uzhhorod National University, 46 Pidhirna Str., 88000 Uzhhorod, Ukraine

<sup>d</sup>Vlokh Institute of Physical Optics, 23 Dragomanov Str., 79005 Lviv, Ukraine

<sup>e</sup>Faculty of Mathematics and Natural Sciences, University of Rzeszów, S. Pigonia 1, PL-35959 Rzeszów, Poland

<sup>f</sup>Semiconductor Physics, Chemnitz University of Technology, D-09107 Chemnitz, Germany

Investigations on the electronic and optical properties of a TlInS<sub>2</sub> layered crystal in the framework of density functional theory were carried out. The electronic band spectrum and the partial density of states were calculated including the dispersion correction. The impact of  $+U$  correction term on the bandgap values was analyzed as well. Based on the band structure calculations, optical characterisation was made for the first time for TlInS<sub>2</sub>, such as the real and imaginary parts of the dielectric function, the refractive index, and the absorption coefficient. Theoretical results of dielectric function and refractive index were compared to the measurement results.

DOI: [10.12693/APhysPolA.136.640](https://doi.org/10.12693/APhysPolA.136.640)

PACS/topics: 61.82.Fk, 71.15.Mb, 78.20.Ci

## 1. Introduction

Recently layered crystals have attracted research interest due to their promising structural and physical properties. A possibility to create new multifunctional artificial materials obtained through the arrangement of several layered crystals has become a new subject of studies [1]. At the stage of looking for new materials, extensive studies are carried out on the structural and physical properties of layered semiconductors. They can be promising candidates for van der Waals heterostructures. One of such materials is TlInS<sub>2</sub>. It belongs to the A<sup>III</sup>B<sup>III</sup>C<sub>2</sub><sup>VI</sup> group of chalcogenide semiconductors — ferroelectrics and is regarded to be a highly anisotropic crystal. It was grown for the first time by Offergeld [2]. TlInS<sub>2</sub> possesses both high- ( $\beta$ ) and low- ( $\alpha$ ) temperature phases [3]. The growth and optical properties of the high-temperature phase of TlInS<sub>2</sub> crystal were described in [4]. The optical band gaps (direct  $E_g^d = 2.33$  eV and indirect  $E_g^{ind} = 2.28$  eV) were measured experimentally [5], while in [6] the electrical conductivity and absorption coefficients as a function of temperature were investigated. The electrical measurements show a strong anisotropy of the conductivity, which is rather temperature independent. The presence of an excitonic peak was registered at 2.58 eV, and the spin-orbit splitting of the valence band at the  $\Gamma$  point at 2.87 eV was observed at 10 K.

First-principle calculation of the electronic structure of TlInS<sub>2</sub> crystal was presented for the first time in [7]. They were using the local density approximation (LDA) and spin-polarized generalized gradient approximation (SGGA) functional with the account of spin-orbit interaction, and only the energy band spectra and values of the effective mass tensor components were calculated.

In the case of the TlInS<sub>2</sub> crystal, it possesses a van der Waals gap (vdW) [2] between its layers. For a more adequate description of its physical properties, the combination of density functional theory and dispersion correction (DFT-D) approach should be taken into account. Since the ordinary DFT usually underestimates the bandgap, the DFT+ $U$  approach will be used instead, to obtain the correct values comparable with the experimental data.

## 2. Lattice parameters of the TlInS<sub>2</sub> crystal and calculation details

TlInS<sub>2</sub> crystallizes in a centered monoclinic lattice structure with  $C2/c$  ( $C_{2h}^6$ ) space symmetry group and exhibits four formula units per primitive cell, that contains 32 atoms. The experimental primitive cell parameters of TlInS<sub>2</sub> [8] are:  $a = 7.72390$  Å,  $c = 15.18650$  Å,  $\alpha = \beta = 97.5481^\circ$ ,  $\gamma = 89.5861^\circ$ . Figure 1 presents the primitive unit cell of a TlInS<sub>2</sub> crystal.

Calculations of the band structure, the electron density of states, real and imaginary parts of the dielectric function, and the absorption coefficient for different polarizations along crystal axes were performed for

\*corresponding author; e-mail: [tanya.babuka@gmail.com](mailto:tanya.babuka@gmail.com)

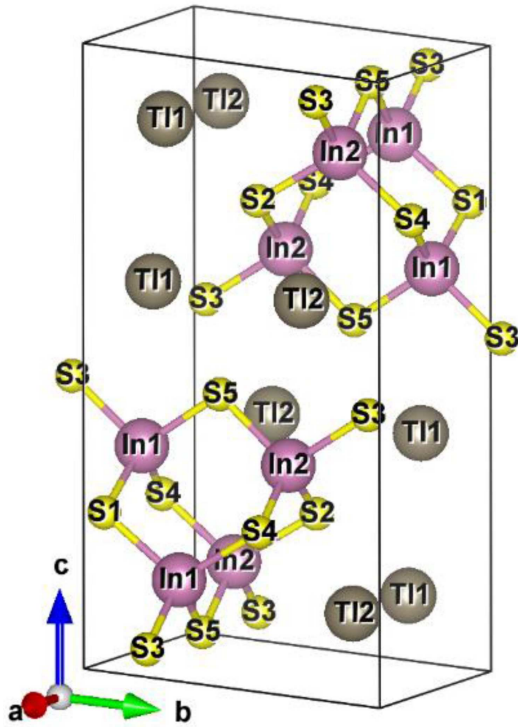


Fig. 1. Primitive cell of a  $\text{TlInS}_2$  crystal.

$\text{TlInS}_2$ . We used the DFT-based Quantum-ESPRESSO program package [9]. Since the  $\text{TlInS}_2$  crystal possesses a layered structure with a vdW gap, the DFT-D approach was applied, taking into account the Tkatchenko and Scheffler (TS) correction [10] of the dispersion interaction. Further, the electronic configurations that were considered were: Tl —  $5d^{10}6s^26p^1$ , In —  $4d^{10}5s^25p^1$ , S —  $3s^23p^4$ . The core electrons were described by means of the ultrasoft Vanderbilt pseudopotentials [11], while the exchange-correlation functional was used in the general gradient approximation (GGA) with the Perdew, Burke, and Ernzerhof (PBE) parametrization [12]. The plane-wave cutoff energy in the self-consistent field (SCF) calculations was selected such that the convergence in the total unit-cell energy was not worse than  $5 \times 10^{-6}$  eV/atom, and it was equal to 300 eV. The Monkhorst–Pack  $\mathbf{k}$ -points grid sampling was set at  $4 \times 4 \times 2$  points for the Brillouin zone [13].

### 3. First-principle calculation results of the electronic properties of $\text{TlInS}_2$ crystal

To explain physical properties of a layered semiconductor  $\text{TlInS}_2$ , we calculated its electronic band structure and partial density of states (pDOS). To this we have applied the DFT-D and DFT(D)+ $U$  approaches. The simulation was carried out for fully geometry optimized structure, i.e., the lattice parameters and atomic positions were relaxed under preserved symmetry. As was

shown already in previous papers concerning materials characterized by a vdW gap [14–16], the inclusion of the dispersion correction in the DFT calculations gives a possibility to describe in a correct way interlayer distances. As a result, the obtained relaxed  $\text{TlInS}_2$  structural parameters are as follows,  $a = b = 7.783385$  Å,  $c = 15.267074$  Å,  $\alpha = \beta = 96.882950^\circ$ ,  $\gamma = 90.035269^\circ$ ,  $V = 911.507392$  Å<sup>3</sup>. They are in a good agreement with experimental data [8].

The first calculation of the  $\text{TlInS}_2$  band structure using the LDA functional was reported by Ismayilova and Orudzhev [7]. In that paper, underestimated values of the bandgap (1.43 eV and 1.25 eV) were obtained by the HGH and FHI pseudopotentials, respectively. The results were consistent with the DFT methodology. From our calculations it follows that  $\text{TlInS}_2$  is a direct bandgap semiconductor with the gap edges localized at the  $\Gamma$  high symmetry point. The value of the direct energy gap obtained in DFT-D approach  $E_g = 1.37$  eV is also significantly smaller than the available experimental estimation of the optical gap ( $\approx 2.33$  eV [5]).

For other ferroelectric chalcogenide semiconductor [17], it has been shown that the DFT+ $U$  approach [18] can lead to a correct description of energy bandwidth. Hence, we applied this approach for  $\text{TlInS}_2$ . When the  $U$  correction was included for  $d$ -states of Tl and In atoms, no significant changes of the bandgap values were observed. This is an expected result, since strongly correlated  $d$ -states are located in very deep energy regions ( $d$ -states of Tl at  $-10$  eV and  $d$ -states of In at  $-15$  eV). Next, the parameter of the Coulomb repulsion  $U = 5$  eV was applied for  $p$ -states of S atoms. In this case, the obtained values of bandgap ( $E_{g(\text{theor})} = 2.296$  eV) were closer to experimental data ( $E_{g(\text{exp.})} = 2.33$  eV [5]) (see Fig. 2).

Furthermore, we calculated for the first time the partial density of states in the DFT(D)+ $U$  approach. The results are presented in Fig. 3.

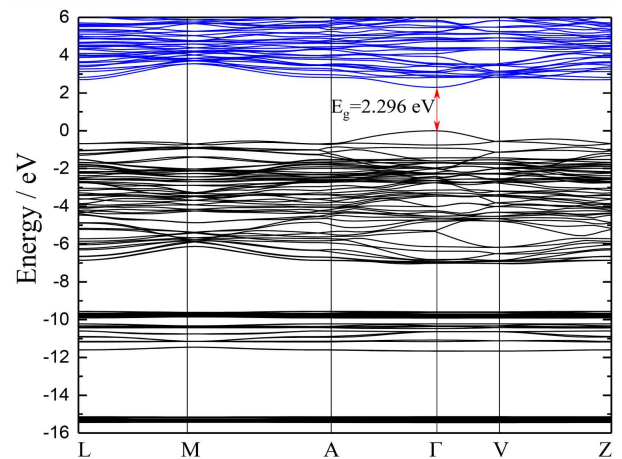


Fig. 2. Electronic band structure of a  $\text{TlInS}_2$  crystal obtained in DFT(D)+ $U$  approach.

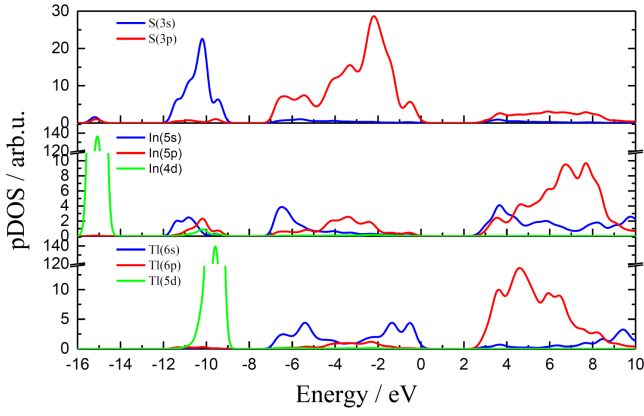


Fig. 3. The DFT(D)+ $U$  partial densities of states (pDOS) of a TlInS<sub>2</sub> crystal.

As can be seen from Figs. 2 and 3, the top of the valence band is formed by  $p$ -states of sulfur, while the bottom of the conduction band is created mainly by  $p$ -states of all TlInS<sub>2</sub> atoms with admixture of In  $s$ -states. The valence band range from  $-16$  eV up to  $0$  eV can be separated into four subbands. The subband deepest in energy ( $-16, -14$ ) eV is built of  $d$ -states of indium. The next subband, covering the energy region from  $-12$  up to  $-7.5$  eV, consists of sulfur  $s$ -states and  $d$ -states of thallium. As reported for TlGaSe<sub>2</sub> [19], the Tl  $5d$  states also contribute to a low-energy peak of pDOS around  $-10$  eV (see Fig. 3). The third subband in the range from  $-7$  to  $-5$  eV originates from  $p$ -states of S and  $s$ -states of In and Tl atoms. The last subband between  $-5$  and  $0$  eV exhibits a strong contribution of S  $p$ -states hybridized with  $p$ -states of indium and thallium atoms.

#### 4. Optical properties of the TlInS<sub>2</sub> crystal

Next, we investigated the optical properties of TlInS<sub>2</sub> within the DFT approach, taking into account the Kramers–Krönig relations [20, 21]. The spectral dependences of the TlInS<sub>2</sub> optical characteristics for different photon polarizations are presented in Figs. 4–6. It should be noted that the energy dependences for unpolarized light and for the polarizations  $E \parallel x$  and  $E \parallel y$  as well, completely coincide due to their symmetry.

The absorption spectra for different polarizations calculated within the DFT/PBE-D(TS) approach are presented in Fig. 4. Our first-principles calculation indicates that TlInS<sub>2</sub> is a direct bandgap crystal with a gap value of  $2.296$  eV. This feature can be validated either by a comparison of calculated values (the band structure in Fig. 2) of the direct and indirect optical gaps (see Fig. 4), as well as of the experimental results [5]. Theoretical energy dependence results of the light absorption coefficient  $\alpha$ ,  $(\alpha \times h\nu)^2$ , and  $(\alpha \times h\nu)^{1/2}$  are presented in Fig. 4. A rough estimation of the indirect and direct optical gaps with the use of simple parabolic model leads to  $E_{g(\text{theor})}^{\text{ind}} = 2.11$  eV and  $E_{g(\text{theor})}^{\text{d}} = 1.82$  eV values.

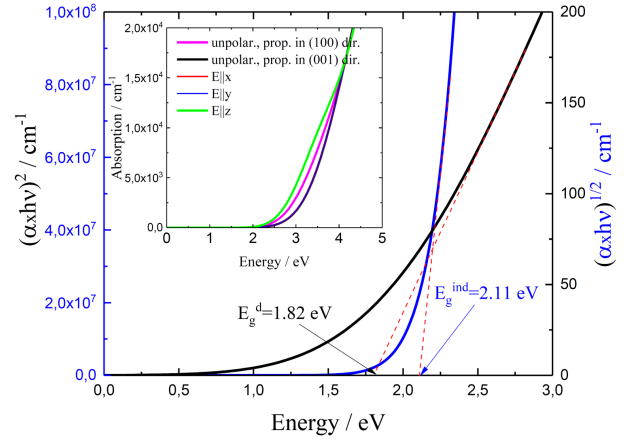


Fig. 4. Theoretically calculated absorption coefficients  $\alpha$  (inset) of a TlInS<sub>2</sub> crystal, as well as  $(\alpha \times h\nu)^2$  and  $(\alpha \times h\nu)^{1/2}$  curves in the low energy region.

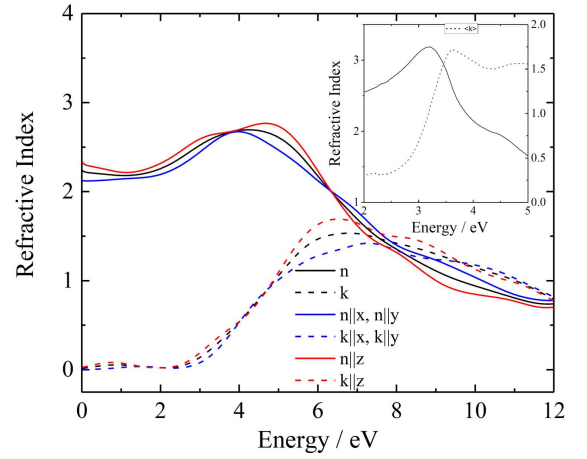


Fig. 5. Theoretically calculated spectral dependences of the refractive indices and extinction coefficients for TlInS<sub>2</sub> crystal (the inset shows our experimental data).

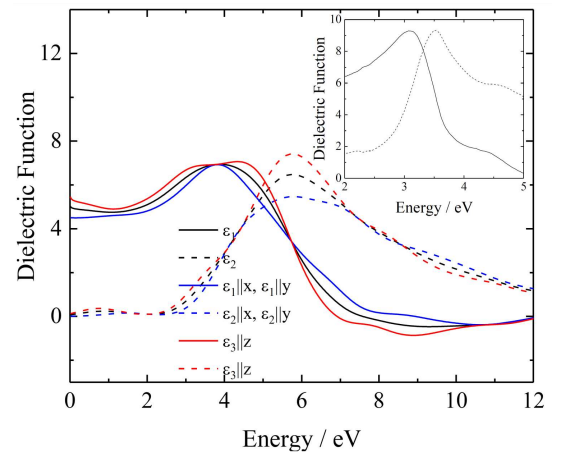


Fig. 6. Theoretically calculated real and imaginary parts of the dielectric function vs. photon energy for TlInS<sub>2</sub> (the inset shows our experimental data).

We have also conducted experimental measurements of the optical properties of TlInS<sub>2</sub>. In particular, single crystals of TlInS<sub>2</sub> were grown by the Bridgman technique [22]. Spectroscopic ellipsometry measurements were carried out using a variable angle spectroscopic ellipsometer J.A. from Woollam Co., Inc. The angle of the incident light beam was adjusted to 70°. As we could not define the  $x$  and  $y$  axes unambiguously, the measurements were made on the layer-plane, i.e., the (001) crystal surface, perpendicular to the optical axis  $c$ . The real ( $\varepsilon_1$ ) and imaginary ( $\varepsilon_2$ ) parts of the effective dielectric function of the TlInS<sub>2</sub> single crystals obtained from experimental measurements, were acquired in the spectral range from 2 to 5 eV.

Theoretical data are presented in Fig. 5. It was found that at the zero energy the refractive indices for TlInS<sub>2</sub> are the following:  $n_{(\text{theor})} = 2.24$ ,  $n_{x(\text{theor})} = n_{y(\text{theor})} = 2.12$ , and  $n_{z(\text{theor})} = 2.34$ , while  $n_{\text{exp}} \approx 2.85$  [23]. High peaks of the refractive indices ( $n_{(\text{theor})} = 2.69$ ,  $n_{x,y(\text{theor})} \approx 2.67$  and  $n_{z(\text{theor})} \approx 2.76$ ) are observed for unpolarized spectra at the energy  $E_{(\text{theor})} \approx 4.26$  eV, while for polarized at  $E_{(\text{theor})} \approx 3.98$  eV for  $E \parallel x(y)$  and  $E_{(\text{theor})} \approx 4.7$  eV for  $E \parallel z$ . The latter corresponds to the visible spectral region. In our experimental measurement the high peak of the refractive index  $n_{\text{exp}} = 3.18$  was obtained at the energy  $E_{\text{exp}} = 3.17$  eV (see an inset in Fig. 5).

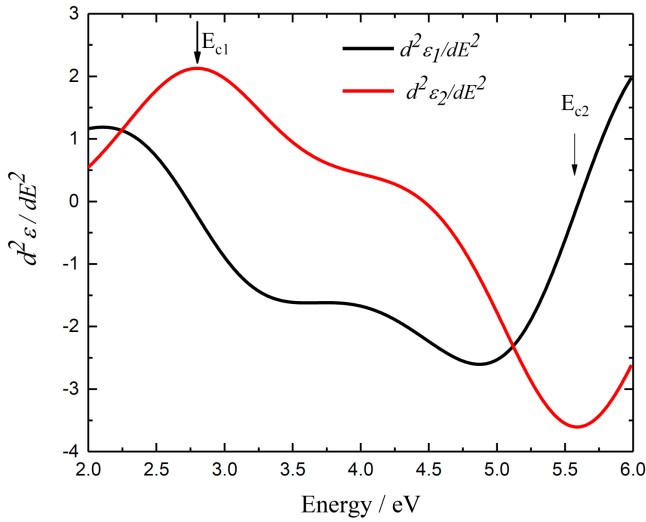


Fig. 7. The second-derivative energy spectra of the components of the TlInS<sub>2</sub> dielectric function.

The maximum value  $\varepsilon_{(\text{theor})}(\omega) = 6.94$  was found at  $E \approx 3.93$  eV,  $\varepsilon_{1x(\text{theor})}(\omega) = 6.92$  at  $E \approx 3.82$  eV and  $\varepsilon_{1z(\text{theor})}(\omega) = 7.06$  at  $E_{(\text{theor})} = 4.33$  eV. As one can see in the inset of Fig. 6, the experimental maximum value  $\varepsilon_{(\text{exp})}(\omega) = 9.28$  was observed at  $E_{(\text{exp})} = 3.1$  eV. Meanwhile, in [24], the maximum value  $\varepsilon_{(\text{exp})}(\omega)$  was found to be 12.51. Other values of the static dielectric constants were reported by Kalomiros and Anagnostopoulos [25] ( $\varepsilon_{1x(\text{exp})}(\omega) = 6.4$ ,  $\varepsilon_{1z(\text{exp})}(\omega) = 7.2$ ) and

were based on ellipsometric measurements. Our first-principles calculations (at  $E_{(\text{theor})} = 0$ ) reported that the static dielectric constants are equal to  $\varepsilon_{(\text{theor})}(0) \approx 5.02$  for unpolarized spectra,  $\varepsilon_{1x(\text{theor})}(0) \approx 4.51$  for the photon polarization  $E \parallel x(y)$ , and  $\varepsilon_{1z(\text{theor})}(0) \approx 5.46$  for  $E \parallel z$ . As shown in Fig. 5, a very slight anisotropy ( $n_{zz}(0)/n_{xx}(0) \approx 1.03$ ) was found for these optical parameters. A similar anisotropy is observed for the real part of the dielectric function ( $\varepsilon_{1z}(0)/\varepsilon_{1x}(0) \approx 1.21$ ).

The obtained dielectric spectra can be used to find the critical point energies ( $E_{\text{cp}}$ ). This critical point energies  $E_{\text{cp}}$  corresponding to interband transitions in TlInS<sub>2</sub> were considered in [26]. The results at room temperature, namely  $E_{c1(\text{exp})} = (3.24 \pm 0.01)$  eV,  $E_{c2(\text{exp})} = (3.33 \pm 0.01)$  eV,  $E_{c3(\text{exp})} = (3.59 \pm 0.01)$  eV, and  $E_{c4(\text{exp})} = (4.52 \pm 0.05)$  eV were obtained in [26] based on the experimentally measured dielectric function. We performed similar calculations of the critical point energies, based on the theoretical value of the dielectric function. For this purpose, we utilized the second derivative spectra of the components of the dielectric function with respect to energy. Figure 7 presents the related spectra for  $\varepsilon_1$  and  $\varepsilon_2$  of TlInS<sub>2</sub>.

Typically, second-derivative spectra are related to the photon energy  $E$ , amplitude  $A$ , critical point energy  $E_{\text{cp}}$ , broadening parameter  $\Gamma$ , and phase angle  $\phi$ . The graphs of second-derivative spectra were smoothed using low-level binomial filtering. The fitting processes were accomplished in the energy range (2–5 eV) in which the smoothed results do not deviate from the experimental data. As a result of calculations, the following values were obtained:  $E_{c1(\text{theor})} = 2.83$  eV,  $E_{c2(\text{theor})} = 5.57$  eV. Taking into account the band structure (Fig. 2), the revealed critical point energies may be associated with band-to-band transitions from  $2p$  sulfur states at the top of the valence band to the  $5p$  thallium states in the bottom of the conduction band.

The description of the optical properties of TlInS<sub>2</sub> and their comparison with experimental data presented in this work has been done for the first time. We should underline that the most accurate, but also very computationally expensive way to simulate optical properties is to solve the Bethe–Salpeter equation [27]. A perfect agreement between theory and experiment can only be achieved considering the electron–hole interaction (excitons), especially if the system is a semiconductor or, an insulator. The Bethe–Salpeter approach which is proved to be very successful for the calculation of absorption spectra of a large variety of systems will be used elsewhere in the future investigation of the optical properties of TlInS<sub>2</sub> crystals.

## 5. Conclusions

In this work, the energy band spectra and partial densities of states of a layered TlInS<sub>2</sub> crystal were obtained using the DFT approach with a dispersion correction. It was shown that interlayer distances in TlInS<sub>2</sub> are well

described only when the vdW correction is included. This is an important aspect for future investigations of its vibrational properties. Additionally, for a correct description of the bandgap value, the DFT/PBE-D(TS)+*U* approach was applied. Next, the following optical properties: refractive indices, dielectric constants, and absorption coefficients were calculated for the first time for TlInS<sub>2</sub>. Our theoretical calculations were supplied with the experimental results of ellipsometric measurements of the dielectric constants and refractive index of TlInS<sub>2</sub>. A comparison of theoretical and experimental data concerning the optical properties of TlInS<sub>2</sub> demonstrates a good agreement.

### Acknowledgments

O.O. Gomonnai gratefully acknowledges Deutscher Akademischer Austauschdienst for the financial support of his research stay at Technische Universität Chemnitz (project No. A/12/85971). M. Sznajder acknowledges the support from the Centre for Innovation and Transfer of Natural Sciences and Engineering Knowledge at the University of Rzeszów.

### References

- [1] A. Geim, I. Grigorieva, *Nature* **499**, 419 (2013).
- [2] G. Offergeld, *U.S. Patent* **3**, 110, 685 (1963).
- [3] G.D. Guseinov, E. Mooser, E.M. Kerimova, R.S. Gamidov, I.V. Alekseev, Z. Ismailov, *Phys. Status Solidi B* **34**, 33 (1969).
- [4] T.J. Isaacs, J.D. Feichtner, *J. Solid State Chem.* **14**, 260 (1975).
- [5] M. Haniias, A. Anagnostopoulos, K. Kambas, J. Spyridelis, *Physica B: Condensed Matter* **160**, 154 (1989).
- [6] M. Haniias, A. Anagnostopoulos, K. Kambas, J. Spyridelis, *Mater. Res. Bull.* **27**, 25 (1992).
- [7] N.A. Ismayilova, H.S. Orudzhev, *Metallofiz. Noveishie Tekhnol.* **38**, 1019 (2016).
- [8] K.J. Range, G. Engert, W. Muller, A. Weiss, *Zeitschrift für Naturforschung B* **29**, 181 (1974).
- [9] P. Giannozzi, S. Baroni, N. Bonini, et al., *J. Phys. Condens. Matter* **21**, 395502 (2009).
- [10] A. Tkatchenko, M. Scheffler, *Phys. Rev. Lett.* **102**, 073005 (2009).
- [11] D. Vanderbilt, *Phys. Rev. B* **41**, 8412 (1990).
- [12] J. Perdew, K. Burke, M. Ernzerhof, *Phys. Rev. Lett.* **77**, 3865 (1996).
- [13] H. Monkhorst, J. Pack, *Phys. Rev. B* **13**, 5188 (1976).
- [14] T. Babuka, K. Glukhov, Y. Vysochanskii, M. Makowska-Janusik, *RSC Adv.* **8**, 6965 (2018).
- [15] T. Babuka, K. Glukhov, Y. Vysochanskii, M. Makowska-Janusik, *Phase Transit.* **92**, 440 (2019).
- [16] L.Y. Kharkhalis, K.E. Glukhov, T.Y. Babuka, M.V. Liakh, *Phase Transit.* **92**, 451 (2019).
- [17] T. Babuka, K.E. Glukhov, Y. Vysochanskii, M. Makowska-Janusik, *RSC Adv.* **7**, 27770 (2017).
- [18] M. Cococcioni, S. de Gironcoli, *Phys. Rev. B* **71**, 035105 (2005).
- [19] N.A. Ismayilova, S.H. Jabarov, *J. Optoelectron. Adv. Mater.* **11**, 353 (2017) ( Rapid Communications).
- [20] A.J. Read, R.J. Needs, *Phys. Rev. B* **44**, 13071 (1991).
- [21] E.D. Palik, *Handbook of Optical Constants of Solids*, Academic Press, Orlando 1985.
- [22] A. Gomonnai, I. Petryshynets, Y. Azhniuk, O. Gomonnai, Y. Roman, I. Turok, A. Solomon, R. Rosul, D.R.T. Zahn, *J. Cryst. Growth* **367**, 35 (2013).
- [23] N.M. Gasanly, *J. Optoelectron. Adv. Mater.* **13**, 49 (2011).
- [24] M.M. El-Nahass, M.M. Sallam, *Egypt. J. Solids* **31**, 31 (2008).
- [25] J.A. Kalomirois, A. Anagnostopoulos, *Phys. Rev. B* **50**, 7488 (1994).
- [26] O. Gomonnai, O. Gordan, P. Guranich, P. Huranich, A. Slivka, A. Gomonnai, D.R.T. Zahn, *J. Nano-Electron. Phys.* **9**, 05025 (2017).
- [27] E.E. Salpeter, H.A. Bethe, *Phys. Rev.* **84**, 1232 (1951).